

Reticle defect sizing of optical proximity correction defects using SEM imaging and image analysis techniques

Larry Zurbrick^a, Lantian Wang^a, Paul Konicek^b, Ellen Laird^b

a - KLA-Tencor Corporation, San Jose, CA

b - VLSI Standards Corporation, San Jose, CA

ABSTRACT

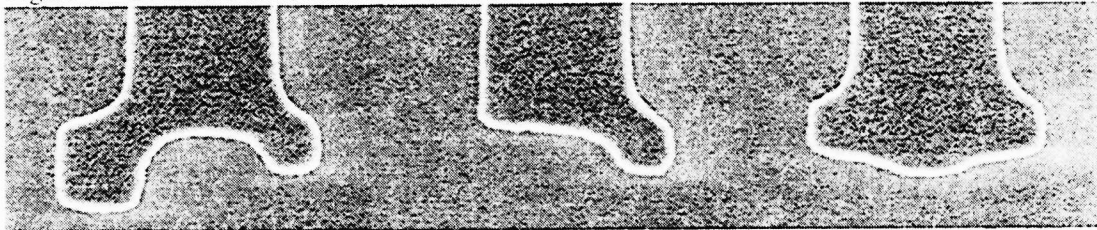
Sizing of programmed defects on optical proximity correction (OPC) features is addressed using high resolution scanning electron microscope (SEM) images and image analysis techniques. A comparison and analysis of different sizing methods is made. This paper addresses the issues of OPC defect definition and discusses the experimental measurement results obtained by SEM in combination with image analysis techniques.

Keywords: OPC, defect measurement, defect printability

1. INTRODUCTION

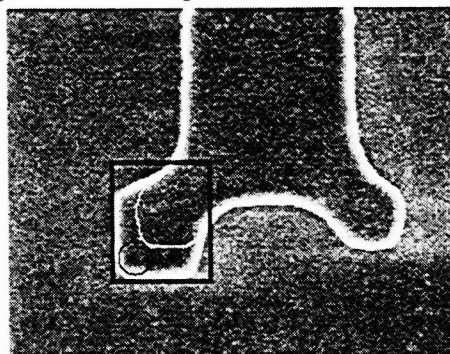
Programmed OPC defect test reticles have been developed¹ in order to assess the performance of automatic defect inspection equipment. **Figure 1** illustrates three different types of programmed defects on serif structures. In order to make quantitative performance measurements of inspection systems, a defect sizing methodology is required. The methodology needs to include definitions of defect size, measurement methods, and a statement of measurement accuracy and precision. Very little attention has been made by the semiconductor industry to the issues and methodology of sizing OPC defects and no definitions exist for OPC defect types such as oversized / undersized / mis-shaped serifs.

Figure 1 – Oversized serif, undersized serif, and filled serif notch defects



Sizing methods for OPC defect types such as oversized serif, undersized serif, and filled serif notch have not been addressed by documents such as SEMI P22-0699, "Guideline for Photomask Defect Classification and Size Definition". From the SEMI P22-0699 document, one may try to extend the bounding box sizing method for shape type defects to these OPC defect types. Prior work² has described a defect sizing method based upon the maximum diameter of a circle capable of being inscribed into a defect area. See **Figure 2** for examples of the bounding box and maximum inscribed circle methods. A third sizing method is the defect area or the square root of defect area. This method is based upon the area difference between defective and non-defective geometries. For all the sizing methods, a reference non-defective geometry is required in order to determine the shape and extent of the defect.

Figure 2 – Bounding box and maximum inscribed circle diameter



Although the SEMI P22-0699 standard does provide definitions for one method of defect sizing, no recommendation is made for actually making the measurement. That is, no guideline is offered for the measurement tool resolution versus defect size relationship. It is desirable to use an imaging instrument with a resolution at least ten times greater than the smallest defect to be measured. Optical methods lack adequate resolution for defect sizes of interest since the point spread function of available optical microscopes is typically larger than the dimensions of the defects of interest. Atomic Force Microscopes (AFM's) have adequate lateral resolution but exhibit probe tip shape interactions with the sample that may be complicated to remove from the observation. Scanning Electron Microscopes (SEM's) possess adequate lateral resolution and with the introduction of charge control hardware, it is no longer necessary to coat a conductive layer on insulating substrates.

2. DEFECT SIZING USING SEM BASED METHOD

A chrome on quartz test mask was constructed with programmed defects on serif structures. The design mimicked a polysilicon gate level with a nominal linewidth of 780 nm on the mask. Serif geometry was designed so that the serif width was 50% of the linewidth with a 25% area overlap. The programmed defect types included oversized / undersized serifs and a filled notch between the serifs as shown in Figure 1. Programmed defects were incremented by 45 nm in size starting at a defect size of 45 nm. Images of programmed defects were gathered using a KLA-Tencor 8100XP-R CD SEM operating at a magnification of 50KX at a landing energy of 1.2KV. SEM magnification calibration was performed using a chrome on quartz pitch standard. This magnification provides an image resolution of 6.25 nm per pixel. The images were stored as TIF image files and transferred to a separate personal computer where the images were analyzed using custom developed defect sizing software. The defect sizing software detects edges, aligns the defect image edges to a reference image edges, identifies and analyzes the non-matching defect area, and reports the measurements. Since a reference image is utilized, the accuracy of the resulting measurements is dependent in part upon the quality of the geometry chosen as the reference image. Reference image geometry quality depends upon the mask generation process variation across the mask. For the purpose of this work, reference images were gathered within 250 μm of the programmed defect locations.

3. OPC DEFECT SIZING RESULTS

Figures 3, 4, and 5 illustrates a sampling of the three different serif defect types and the results for Maximum Inscribed Circle Diameter (MICD)¹, Square Root Area (SRA) of the actual defect area, and Bounding Box dimension (BB x / y). It can be seen from the graphs in Figure 6, 7, and 8 that the use of the bounding box methods does not provide a uniform or monotonically increasing measurement for oversize and undersized serifs as the size of the defects increase whereas the maximum inscribed circle diameter and square root area methods do. This is due in part to the highly resolved defect shape provided by the SEM images. At the extents of the difference image, the defect may only be a few nanometers in height and tens of nanometers in length which does not significantly affect the SQA or MICD sizes, but is significant in determining bounding box dimensions. Undersized serif defect number 7 in Fig. 7 shows that the bounding box method indicates that the defect has decreased in size as compared to defect number 6 when the defect size has actually increased. This behavior can also be seen in Figs. 6 and 8 for the bounding box X or Y measurements. The geometric average of the X and Y bounding box size (square root of X times Y bounding box sizes) was also briefly investigated, but the non-monotonic sizing behavior persisted. Therefore, the bounding box method is not as sensitive of a measure in showing differences in serif defect size. SRA and MICD methods provide a uniformly increasing size measurement for the three defect types and appear to be correlated for the defect sizes investigated. See Figure 9. For the OPC and other defect types studied, the SRA method always reports a defect size larger than the MICD method. The defect type exceptions to this condition are small pinhole and pindot defect types where the defects tend to print as circles. The MICD sizing method is a measure of the maximum edge displacement for high aspect ratio (>2:1) edge defects where the long axis of the defect is parallel to the geometry edge. The MICD method may be preferable to the SRA method in cases of high aspect ratio edge defects since a small edge displacement over a relatively large distance will produce a relatively large SRA defect size. The MICD method will give the size of the edge displacement, which is more consistent with the accepted method for sizing edge displacement defect.

4. DEFECT PRINTABILITY INVESTIGATION

It was of interest to investigate the correlation between sizing method and defect printability. This was accomplished through resist simulations using Sigma-C's Solid-C software. The SEM images shown in Figs. 3, 4, and 5 were manually converted to CAD layouts and used as the input images for the simulator. Typical DUV process parameters were chosen representative of a polysilicon gate process. See Table 1. Based upon the reticle linewidth of 780 nm, a 180 nm wafer linewidth was targeted assuming a 4x reduction magnification. Since the serif defects would affect Line End Shortening (LES), a reference edge was

included with a database design gap of 260 nm from the line end at wafer scale. A focus/exposure series was performed to determine the process window for the 180 nm line. Critical dimension measurements were made on the simulated 3D developed resist image at 5% remaining resist thickness from the substrate. The 260 nm database design gap resulted in a line end to reference edge gap of 270 nm for the non-defective, reference image in the litho simulation. Results of the simulations are shown in **Figures 10, 11, and 12**. The graphs in Figs. 10, 11, and 12 plot the wafer LES value normalized to the no defect gap versus the reticle defect size by sizing method. It should be noted that the measurement resolution on the 3D resist images is 10 nm due to the simulation tool's measurement resolution on 3D images. This accounts for some of the discontinuities in the plots. For all three defect types, the shapes of the curves are similar between MICD and SRA sizing methods and can be predicted from the correlation between MICD and SRA sizing methods shown in Fig. 9. Negative values of LES indicate the gap between the line end and reference geometry decreased and can be considered as line end lengthening.

Table 1 – Simulation process parameters

Wavelength	248 nm
NA	0.6
Sigma	0.75
Exposure Dose	9.75 mJ/cm ²
Focus offset	-0.30 μ m
Reduction factor	4x
Resist / thickness	APEX-E, 0.83 μ m
Bottom ARC / thickness	ARC11 / 0.12 μ m
Underlying layer	0.30 μ m poly-Si

The correlation of SRA to MICD in predicting defect printability was of interest. **Figure 13** plots LES versus the reticle defect size for the filled serif notch and oversized serif defects. These two defect types were chosen since both increased the amount of attenuating material at the line end and are located within a quarter of the imaging system's point spread function from one another. Note in Fig. 13 that the two defect types affect LES equally and that the data for each defect sizing method is tightly grouped together. This result indicates that the SRA and MICD defect sizing methods provide the same degree of defect printability correlation for the two defect types and sizes investigated.

5. CONCLUSIONS

Defect sizing can be accomplished using SEM based methods on mask substrates without a conductive coating using the KLA-Tencor 8100XP-R CD SEM.

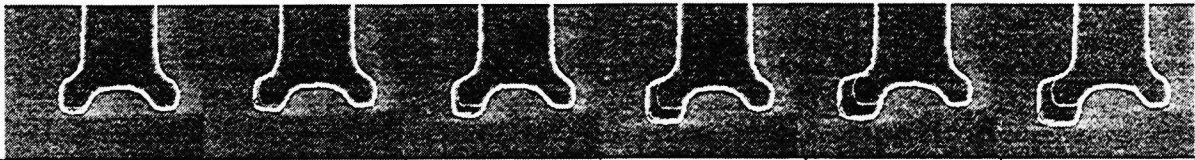
Extensions to the bounding box method are not suitable for sizing defects due to defect artifacts such as "tails" which unfavorably bias the measured defect size. The maximum inscribed circle diameter defect sizing method provides a measure of the maximum edge displacement for high aspect ratio defects.

The Square Root of Area and Maximum Inscribed Circle Diameter methods of defect sizing provide the same degree of defect printability correlation for oversized serifs and filled serif notch defects.

6. REFERENCES

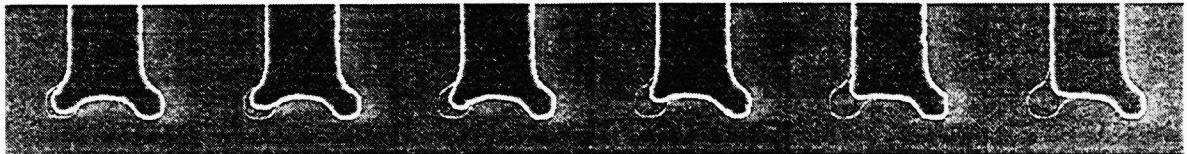
1. L. Zurbrick, "Reticle defects on optical proximity correction features," in *Photomask and X-Ray Mask Technology V*, Naoaki Aizaki, Editor, Proceedings of SPIE Vol. 3412, 471-79 (1998).
2. L. Zurbrick, S. Khanna, J. Lee, J. Greed, E. Laird, R. Blanquies, "Reticle defect size calibration using low-voltage SEM and pattern recognition techniques for sub-200 nm defects," in *19th Annual BACUS Symposium on Photomask Technology*, Frank E. Abboud, Brian J. Grenon, Editors, Proceedings of SPIE Vol. 3873, 651-58 (1999)

Figure 3 – Oversized serif defect



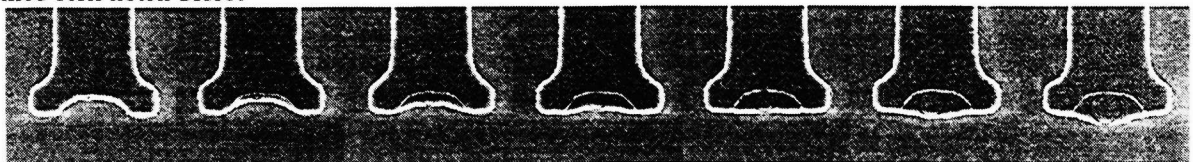
MICD	0.044	0.053	0.094	0.144	0.172	0.197
SRA	0.103	0.150	0.194	0.269	0.301	0.326
BB x / y	0.281 / 0.125	0.300 / 0.338	0.356 / 0.344	0.394 / 0.494	0.456 / 0.444	0.625 / 0.481

Figure 4 – Undersized serif defect



MICD	0.056	0.088	0.116	0.178	0.241	0.278
SRA	0.143	0.179	0.201	0.247	0.281	0.298
BB x / y	0.275 / 0.338	0.325 / 0.294	0.313 / 0.369	0.425 / 0.419	0.463 / 0.519	0.475 / 0.506

Figure 5 – Filled serif notch defect



MICD	0.022	0.056	0.116	0.153	0.194	0.228	0.278
SRA	0.097	0.178	0.239	0.282	0.313	0.340	0.367
BB x / y	0.525 / 0.144	0.588 / 0.150	0.625 / 0.169	0.713 / 0.188	0.719 / 0.194	0.744 / 0.238	0.769 / 0.281

Figure 6 – Oversized serif defect size results

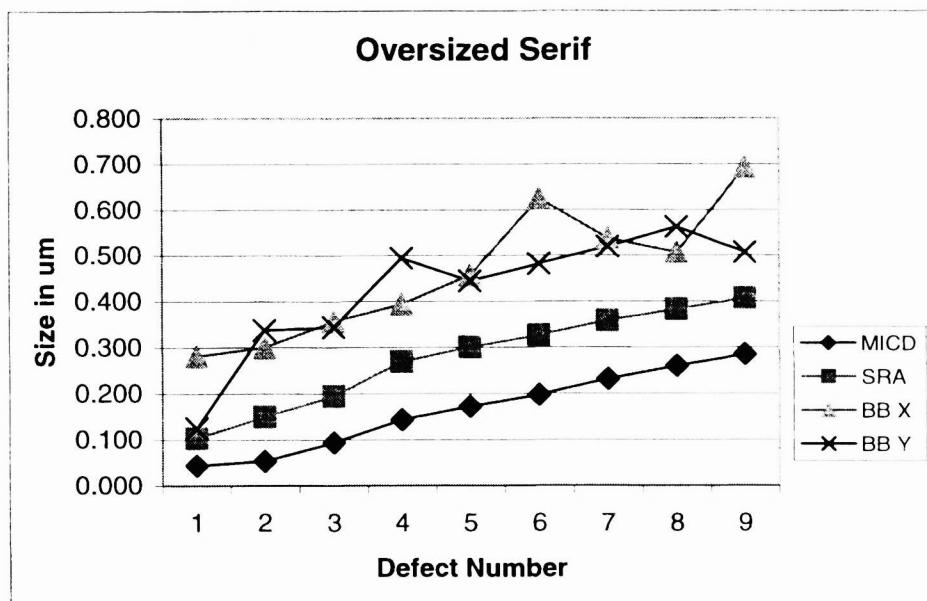


Figure 7 – Undersized serif defect size results

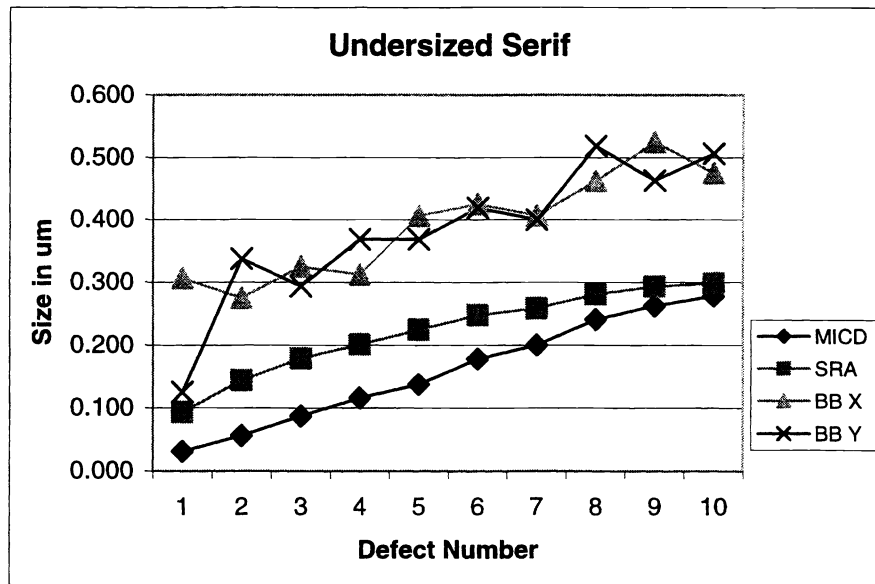


Figure 8 – Filled serif notch defect size results

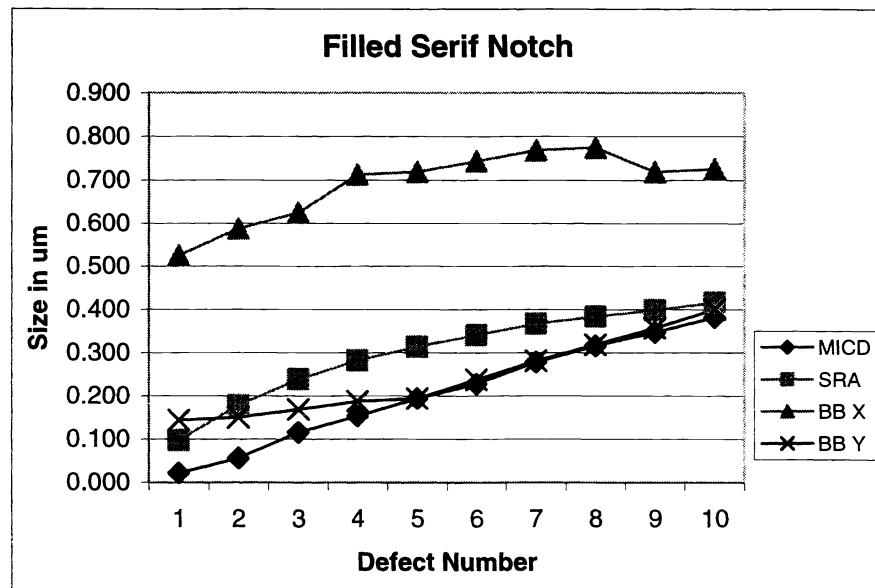


Figure 9 – SRA vs. MICD sizing method correlation

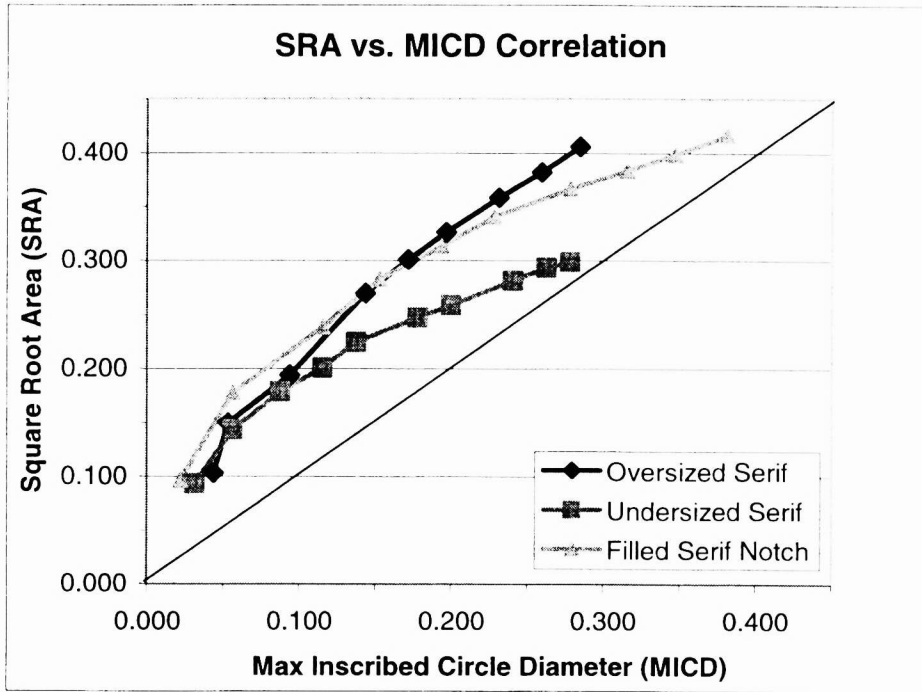


Figure 10 – Oversized serif printability results

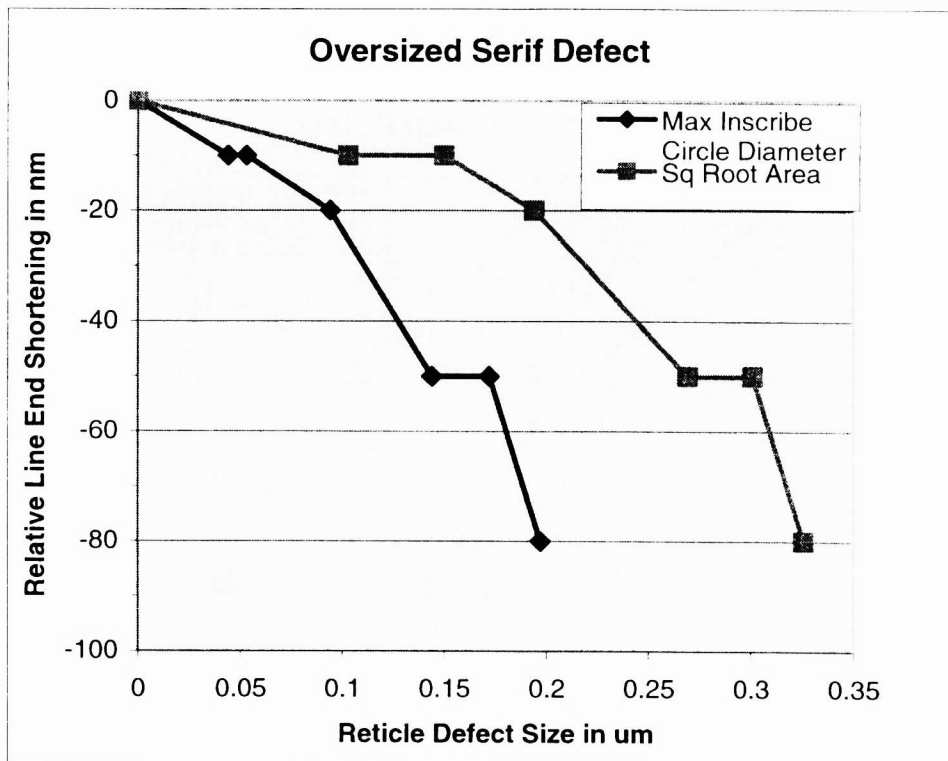


Figure 11 – Undersized serif printability results

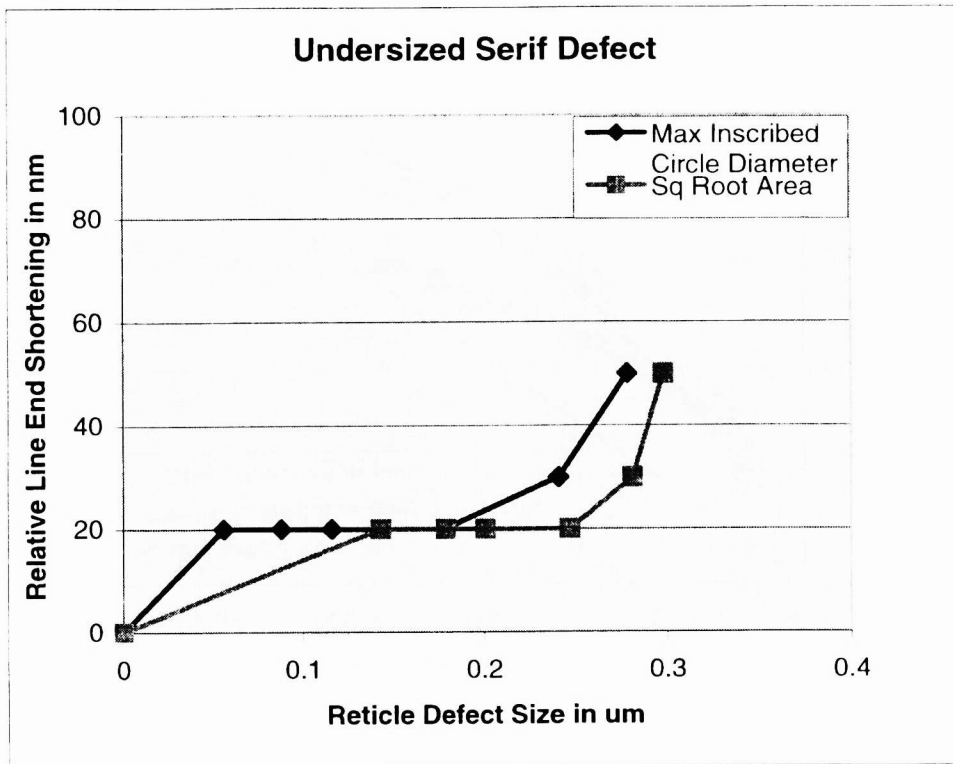


Figure 12 – Filled serif notch printability results

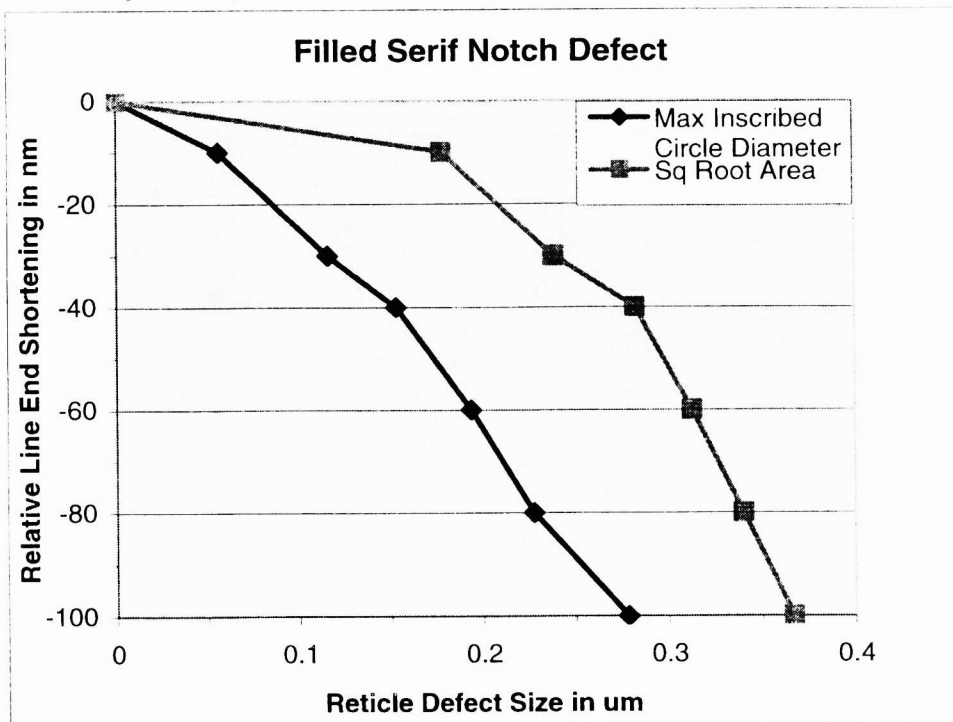


Figure 13 – Defect printability comparison between oversized serif and filled serif notch defects

